MOVING TARGET TRACKING USING TIME REVERSAL METHOD

S. Bahrami[*], A. Cheldavi, and A. Abdolali

Iran University of Science and Technology, Narmak, Tehran 1684613114, Iran

Abstract—Time reversal focusing of electromagnetic waves is investigated in case of source motion. We extract analytical formulation of uniformly moving source in presence of ideal time reversal cavity (TRC) and a more realistic model, time reversal mirror (TRM). Similar to the acoustic case, it has been observed that in case of moving point source spatial focusing is still achievable. Furthermore, we also investigate super resolution effects on time reversal (TR) focusing of moving source in continuous random media. Results shows that an increase in (multipath) leads to better focusing resolution of the time-reversed signals.

1. INTRODUCTION

The concept of Time Reversal Mirror has become a foundation of numerous studies in both acoustics and electromagnetism [1, 2]. The capability of time reversal method in focusing waves attracts many applications ranging from remote sensing, imaging or wireless communication [3–11]. Since the need for tracking of moving targets in strongly cluttered environments arises in many radar applications, including intruder detection systems and through the wall microwave imaging [12–20], the effect of source motion on time reversal focusing is critical. In this paper, we address the problem of time reversal focusing of electromagnetic waves in case of moving source.

Underwater acoustic experiments and theoretical analysis have demonstrated that in case of non stationary source the focusing can still be achieved [21–23]. It was shown that, in the presence of a uniformly-moving point source, focusing of acoustic waves is obtained along the time-reversed trajectory [23]. Based on this result

* Corresponding author: Siroos Bahrami (bahramis@iust.ac.ir).

an approach for handling Doppler shifts in coherent time-reversed underwater communications was proposed [22]. Furthermore, in [24] a single antenna scenario was investigated for multipath compensation in the presence of Doppler shifts due to target motion in a dense multipath environment. In [25] two time-reversal algorithms were introduced for tracking moving targets in clutter. The first algorithm classifies existing scatterers into stationary versus moving targets by means of analyzing multistatic data matrices (MDMs). The second algorithm yields real-time selective tracking of each moving target by means of differential time reversal.

From a theoretical point of view, most prior work on imaging non stationary objects focused on techniques and only a few works are specifically devoted to the theory of time-reversal of electromagnetic waves through disordered media. Recently, De Rosny et al. [26] developed the theory of monochromatic time-reversal mirrors for electromagnetic waves in frequency domain. In this paper we extend the theory to explain the efficiency of time-reversal in case of uniformly moving source. In first step we assume homogeneous background media and time-harmonic fields. However, effects of clutter on TR array performance for moving source have not been considered. Under such conditions, clutter can contaminate transmitted signal, which may mask source position. Effects of background clutter from continuous (inhomogeneous) random media (where volumetric scattering effects are important) on standard TR have been examined for EM waves in [27, 28]. Thus, in next step we address the problem of moving source in continuous random medium and the effects of first and second order random medium statistics on the focusing performance. The investigation is done via numerical simulations employing the finite-difference time-domain (FDTD) method.

The remainder of the paper is organized as follows. In Section 2 the concept of idealized "closed" time reversal mirror, i.e., time reversal cavity is applied to the moving source problem. We then extend the problem to more realistic time reversal array in Section 3. In Section 4, in order to investigate properties of moving point source in continuous random media numerical simulation is performed by means of finite-difference time-domain (FDTD) method as outlined in [27]. Finally, conclusions are drawn in Section 5.

2. MOVING POINT SOURCE IN TR CAVITY

The basis of Time reversal cavity (TRC) concept has been provided both for acoustic and electromagnetic waves [29, 30]. The time domain Green function of time reversed field is driven for scalar waves as

follows,

$$G_{\mathrm{TR}}(r, r_s, t) = G(r, r_s, -t) - G(r, r_s, t) \tag{1}$$

In this equation no reference is made to the closed surface; that is, the field generated by the closed TRC is independent of the size, shape and location of TRC. In [17] the effect of acoustic source motion on focusing has been taken into consideration. For the point source $f(t)$ with constant speed v the time reversed field is

$$\psi_{\mathrm{TR}}(r, t) = \frac{f(\tau_-) - f(\tau_+)}{4\pi R(-t)\sqrt{1 - \beta^2 \sin^2 \theta_{-t}}} \tag{2}$$

where

$$\tau_{\pm} = -t + \gamma^2 R(-t)/c \left(-\beta \cos \theta_{-t} \pm \sqrt{1 - \beta^2 \sin^2 \theta_{-t}} \right) \tag{3}$$

$$\beta = \frac{v}{c}; \quad \gamma = \frac{1}{\sqrt{1 - \beta^2}}. \tag{4}$$

In Equation (2) $R, (t)$ is the distance between source and the observation point at time t, θ_t is the angle between the source velocity vector and the vector connecting the source to the observation point at time t. It can be concluded that the spatial separation between the focal point and the moving source is zero at the instant of transmission that is, the focus occurs at the point of transmission.

In this letter we show that this result can be extended to electromagnetic waves. The electric field obeys vector wave equation

$$\nabla \times \nabla \times \mathbf{E}(\mathbf{r}, t) + \frac{1}{c^2}\frac{\partial^2}{\partial t^2}\mathbf{E}(\mathbf{r}, t) = -\mu\delta(\mathbf{r} - \mathbf{r}_s)\frac{\partial}{\partial t}\mathbf{J}(t) \tag{5}$$

The dyadic Green function obeys a similar equation:

$$\nabla \times \nabla \times \bar{\bar{\mathbf{G}}}(\mathbf{r}, \mathbf{r}'; t) + \frac{1}{c^2}\frac{\partial^2}{\partial t^2}\bar{\bar{\mathbf{G}}}(\mathbf{r}, \mathbf{r}'; t) = -\delta(\mathbf{r} - \mathbf{r}')\delta(t)\bar{\bar{\mathbf{I}}} \tag{6}$$

where $\bar{\bar{\mathbf{I}}}$ is the unit dyadic and the dyadic Green function is expressible in terms of scalar Green function as follow

$$\bar{\bar{\mathbf{G}}}_{\mathrm{ret}}(\mathbf{r}, \mathbf{r}'; t) = \left(\bar{\bar{\mathbf{I}}} - \frac{\nabla\nabla}{c^2 \partial_t^2} \right) g_{\mathrm{ret}}(\mathbf{r}, \mathbf{r}'; t) \tag{7}$$

where g_{ret} is the scalar Green function [31]. In case of free space the scalar Green function has the solution

$$g_{\mathrm{ret}}(\mathbf{r}, \mathbf{r}'; t) = -\frac{\delta(t - |\mathbf{r} - \mathbf{r}'|/c)}{4\pi |\mathbf{r} - \mathbf{r}'|} \tag{8}$$

By introducing dipole moment $\mathbf{p}(t)$ as

$$\mathbf{J}(t) = \frac{\partial}{\partial t}\mathbf{p}(t) \tag{9}$$

The relationship between electric field and initial dipole source, with dipole moment $\mathbf{p}(t)$, located at position $\mathbf{r}_s$ is

$$\mathbf{E}(\mathbf{r}, t) = \mu\frac{\partial^2}{\partial t^2}\int\limits_{R^3}\int\limits_{-\infty}^{+\infty}\bar{\bar{\mathbf{G}}}_{\mathrm{ret}}\left(\mathbf{r}, \mathbf{r}'; t - t'\right)\mathbf{p}\left(t'\right)\delta\left(\mathbf{r}' - \mathbf{r}_s\right)dt'dv'$$

$$= \mu\frac{\partial^2}{\partial t^2}\bar{\bar{\mathbf{G}}}_{\mathrm{ret}}(\mathbf{r}, \mathbf{r}_s; t)_t^*\mathbf{p}(t) \tag{10}$$

In [26], De Rosny et al. showed that dyadic Green function of time reversed vector field has the same form as scalar Green function. In that,

$$\bar{\bar{\mathbf{G}}}_{tr}(\mathbf{r}, \mathbf{r}_s; t) = \bar{\bar{\mathbf{G}}}_{\mathrm{ret}}(\mathbf{r}, \mathbf{r}_s; -t) - \bar{\bar{\mathbf{G}}}_{\mathrm{ret}}(\mathbf{r}, \mathbf{r}_s; t) \tag{11}$$

By introducing the dyadic kernel distribution

$$\bar{\bar{\mathbf{K}}}(\mathbf{r}, \mathbf{r}_s; t) = \left(\bar{\bar{\mathbf{I}}} - \frac{\nabla\nabla}{c^2\partial_t^2}\right)\left[\frac{\delta(t + |\mathbf{r} - \mathbf{r}_s|/c)}{4\pi|\mathbf{r} - \mathbf{r}_s|} - \frac{\delta(t - |\mathbf{r} - \mathbf{r}_s|/c)}{4\pi|\mathbf{r} - \mathbf{r}_s|}\right] \tag{12}$$

Such that the time-reversed electric field in cavity takes a very simple form

$$\mathbf{E}_{tr}(\mathbf{r}, t) = \mu\frac{\partial^2}{\partial t^2}\bar{\bar{\mathbf{K}}}(\mathbf{r}, \mathbf{r}_s; t)_t^*\mathbf{p}(-t) \tag{13}$$

Although, in case of moving source results take different form. The time reversed electric field due to initial dipole source movement with constant velocity v is

$$\mathbf{E}_{tr}(\mathbf{r}, t) = \mu\frac{\partial^2}{\partial t^2}\int\limits_{R^3}\int\limits_{-\infty}^{+\infty}\bar{\bar{\mathbf{K}}}\left(\mathbf{r}, \mathbf{r}'; t - t'\right)\mathbf{p}\left(-t'\right)\delta\left(\mathbf{r} - \mathbf{v}t'\right)dt'dv' \tag{14}$$

Integrating (14) over the co-ordinates yields:

$$\mathbf{E}_{tr}(\mathbf{r}, t) = \mu\frac{\partial^2}{\partial t^2}\int\limits_{-\infty}^{+\infty}\bar{\bar{\mathbf{K}}}\left(\mathbf{r}, \mathbf{v}t'; t - t'\right)\mathbf{p}\left(-t'\right)dt' = \mu\frac{\partial^2}{\partial t^2}\int\limits_{-\infty}^{+\infty}\left(\bar{\bar{\mathbf{I}}} - \frac{\nabla\nabla}{c^2\partial_t'^2}\right)$$

$$\left[\frac{\delta(t - t' + |\mathbf{r} - \mathbf{v}t'|/c)}{4\pi|\mathbf{r} - \mathbf{v}t'|} - \frac{\delta(t - t' - |\mathbf{r} - \mathbf{v}t'|/c)}{4\pi|\mathbf{r} - \mathbf{v}t'|}\right]\mathbf{p}(-t')dt' \tag{15}$$

Using the property of the Dirac delta-function:

$$\delta(F(x)) = \sum_i\frac{\delta(x - x_i)}{|F'(x_i)|} \tag{16}$$

It is reduced to the form

$$\delta(t - t' + |\mathbf{r} - \mathbf{v}t'|/c) = \frac{\delta(t' - \tau_\pm)}{\sqrt{1 - \beta^2 \sin^2 \theta_t}} \qquad (17)$$

where the retarded time $\tau_\pm$ is the solution of the equation:

$$t - \tau - \frac{|\mathbf{r} - \mathbf{v}\tau|}{c} = 0, \qquad (18)$$

From (15) and (17) we have

$$\mathbf{E}_{tr}(\mathbf{r}, t) = \mu \left[\frac{\mathbf{R}(-t) \times \left(\mathbf{R}(-t) \times \frac{\partial^2}{\partial t^2} [\mathbf{p}(\tau_-) - \mathbf{p}(\tau_+)] \right)}{4\pi R(-t) \sqrt{1 - \beta^2 \sin \theta_{-t}}} \right]$$

$$+ \eta \left[\frac{3\mathbf{R}(-t) \left(\mathbf{R}(-t) \cdot \left(\frac{\partial}{\partial t} [\mathbf{p}(\tau_-) - \mathbf{p}(\tau_+)] \right) \right) - \frac{\partial}{\partial t} [\mathbf{p}(\tau_-) - \mathbf{p}(\tau_+)]}{4\pi R^2(-t) \left(1 - \beta^2 \sin \theta_{-t} \right)} \right]$$

$$+ \frac{1}{\varepsilon} \left[\frac{3\mathbf{R}(-t)((\mathbf{R}(-t) \cdot ([\mathbf{p}(\tau_-) - \mathbf{p}(\tau_+)])) - [\mathbf{p}(\tau_-) - \mathbf{p}(\tau_+)]}{4\pi R^3(-t) \left(1 - \beta^2 \sin \theta_{-t} \right)^{3/2}} \right] \qquad (19)$$

where $\mathbf{R}(t)$ is the unit vector between source and the observation point at time t. The first terms in Equation (19) represent "far-field" contribution. The time reversed magnetic field is:

$$\mathbf{H}_{tr}(\mathbf{r}, t) = \frac{\mathbf{R}(-t) \times \frac{\partial^2}{\partial t^2} (\mathbf{p}(\tau_-) - \mathbf{p}(\tau_+))}{4\pi c R(-t) \sqrt{1 - \beta^2 \sin \theta_{-t}}} - \frac{\mathbf{R}(-t) \times \frac{\partial}{\partial t} (\mathbf{p}(\tau_-) - \mathbf{p}(\tau_+))}{4\pi R^2(-t)(1 - \beta^2 \sin \theta_{-t})} \quad (20)$$

Equations (19) and (20) show that in the presence of a uniformly-moving dipole source, electromagnetic field focusing only obtained when $R(-t) = 0$, i.e., along the time-reversed trajectory. Previous result can be best illustrated by the visualization of the time-domain progress of the backward propagations as in Fig. 1. The numerical computation is performed with a TRC made of 40 dipoles uniformly distributed over a 16 wavelength radius circle. The initial source, a uniformly moving dipole with constant velocity $v = c/10$ in $-y$ direction, is at center of the circle and its polarization is perpendicular to circle plane. The simulation is carried out using FDTD. In first step the electric fields were recorded at the array antennas of TRC. Then time-reversed fields are transmitted back into the same homogeneous medium.

In Fig. 1 the snapshots of the electric field ($\mathbf{E}_z$) propagation in discrete TRC taken at different times are shown for backward propagation. As can be seen in snapshots before spatial focusing, the wave front intensity is localized in $-y$ direction due to Doppler effect. This phenomenon is visible in subsequent snapshots but in
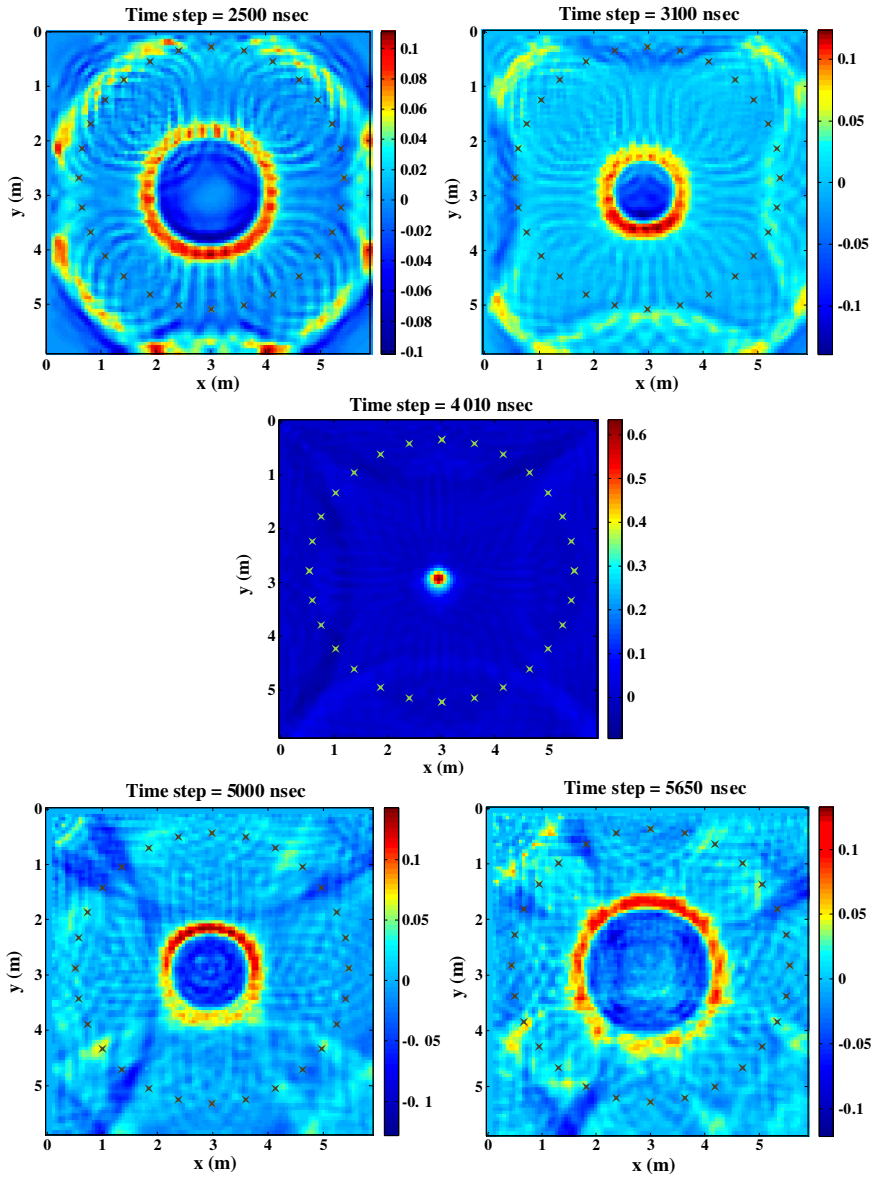
Figure 1. Snapshots of the backward electric field component (E_z) propagation when the time reversed fields recorded at the array antennas of TRC are transmitted back into the same homogeneous medium. At $t = 4010$ nsec, focusing around the original source location occurs.
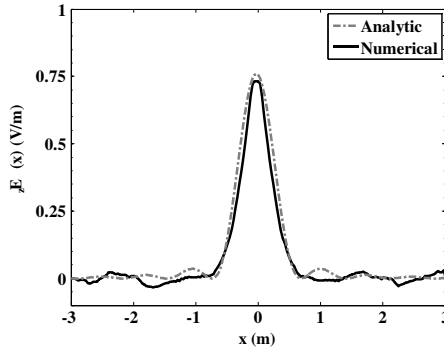
Figure 2. Amplitude of the z-component of the time reversed electric field with respect to the distance to the initial moving dipole source along the x-axis. The continuous line corresponds to the numerical (2D-FDTD) TRC simulation made of 40 emitters uniformly distributed on a 16-wavelength radius sphere and the dashed line corresponds to analytical formulation.

opposite direction. It is observed that although only a limited number of antennas (40 dipoles) is used to receive and record the propagating signals, it is enough for the back propagated signals to focus around the moving point source initial location and the focusing spot size is dictated by the classical diffraction limit [32]. Fig. 2 illustrates time reversed electric field with respect to the distance to the initial moving dipole source along the x-axis. According to Fig. 2 there is a good agreement between numerical simulation and analytical formulation.

3. MOVING POINT SOURCE IN TR MIRROR

We have developed the concept of TRC in order to provide a better understanding of the time reversal focusing in presence of moving point source. A cavity as described above cannot be realized experimentally. Therefore, in this section we extend the concept to a more realistic model, i.e., time reversal mirror.

Consider a single target is moving with a constant velocity v. Assume a linear array of $\mathbf{K}$ receivers, the ith receiver located at $\mathbf{r}_i$, and a time domain pulse $p_s(t)$, dipole moment, is emitted from sth transmitter at $\mathbf{r}_s$.

The electric fields incident on the target at $\mathbf{r}$ due to the source are represented as:

$$\mathbf{E_i}(\mathbf{r}, t) = \mu \frac{\partial^2}{\partial t^2} \sum_{s=1}^{\mathbf{K}} \bar{\bar{\mathbf{G}}}_{\mathrm{ret}}(\mathbf{r}, \mathbf{r}_s; t)_t^* \mathbf{p}_s(t) \tag{21}$$

In case of point like target it can be characterized by an equivalent current (dipole) element

$$\mathbf{J_V}(\mathbf{r}, t) = \frac{\partial}{\partial t} \mathbf{p_V}(\mathbf{r}, t) = (\varepsilon - \varepsilon_0) \frac{\partial}{\partial t} \mathbf{E_i}(\mathbf{r_0}(t), t) \delta(\mathbf{r} - \mathbf{r_0}(t)) \quad (22)$$

where,

$$\mathbf{r_0}(t) = \mathbf{v}t. \quad (23)$$

The backscattered field incident on the ith antenna is:

$$\mathbf{E}_s(\mathbf{r_i}, t) = \mu \frac{\partial}{\partial t} \bar{\bar{\mathbf{G}}}_{\text{ret}}(\mathbf{r_i}, \mathbf{r_0}(t); t)_{\mathbf{t}}^* \mathbf{J_V}(t) = \mu \frac{\partial^2}{\partial t^2} \bar{\bar{\mathbf{G}}}_{\text{ret}}(\mathbf{r_i}, \mathbf{r_0}(t); t)_{\mathbf{t}}^* \mathbf{p_V}(t) \quad (24)$$

$$\mathbf{E}_s(\mathbf{r_i}, t) = \mu \frac{\partial^2}{\partial t^2} \int\limits_{-\infty}^{+\infty} \bar{\bar{\mathbf{G}}}_{\text{ret}}(\mathbf{r_i}, \mathbf{r_0}(t'); t - t') \mathbf{p_V}(t') dt' \quad (25)$$

By assuming that the target is far from time reversal mirror far field approximation can be used:

$$\mathbf{E}_s(\mathbf{r_i}, t)_{\text{farfield}} = \mu \left[\frac{\mathbf{R_i}(t) \times \left(\mathbf{R_i}(t) \times \frac{\partial^2}{\partial t^2} \mathbf{p_v}(t_r) \right)}{4\pi R_{\mathbf{i}}(t) \sqrt{1 - \beta^2 \sin \theta_t}} \right] \quad (26)$$

where $\mathbf{R_i}(t)$ is the unit vector connecting moving point source and receiver located at $\mathbf{r_i}$. t_r is the retarded time obtained by solving Equation (18). Now time reversed fields recorded at the array antennas of TRM are transmitted back and the time-reversed source distribution becomes

$$\mathbf{J_i}(\mathbf{r}, t) = \frac{\mathbf{E}_s(\mathbf{r_i}, -t)}{\eta} \delta(\mathbf{r} - \mathbf{r_i}) \quad (27)$$

The backward electric field propagating due to TRM radiation is:

$$\mathbf{E}_{tr}(\mathbf{r}, t) = \frac{1}{c} \frac{\partial}{\partial t} \sum_{s=1}^{K} \bar{\bar{\mathbf{G}}}_{\text{ret}}(\mathbf{r}, \mathbf{r_i}; t)_t^* \mathbf{E}_s(\mathbf{r_i}, -t) \quad (28)$$

In the far-field:

$$\mathbf{E}_{tr}(\mathbf{r}, t)_{\text{farfield}} = \frac{\mathbf{R}(t) \times \left(\mathbf{R}(t) \times \frac{\partial}{\partial t} \mathbf{E}_s(\mathbf{r_i}, -t) \right)}{4\pi c R(t)}$$

$$= \mu \frac{\mathbf{R} \times \left[\mathbf{R} \times \left\{ \mathbf{R_i}(-t + R/c) \times \left[\mathbf{R_i}(-t + R/c) \times \frac{\partial^3}{\partial t^3} \mathbf{p}(t_r(-t + R/c)) \right] \right\} \right]}{(4\pi)^2 c R R_{\mathbf{i}}(-t + R/c) \sqrt{1 - \beta^2 \sin \theta_{-t + R/c}}} \quad (29)$$

where $\mathbf{R}(t)$ is the unit vector between transmitter located at $\mathbf{r_i}$ and observation point. Again it can be observed that the electromagnetic field focusing only obtained along the time-reversed trajectory.

4. MOVING POINT SOURCE IN RANDOM MEDIUM

A uniformly moving electric dipole and a linear array of electric dipoles are located in a lossless random medium with spatially fluctuating relative permittivity as introduced in [27]. The random medium is characterized by correlation length (l_s) and variance (δ), and is generated using the procedure discussed in [33]. At each point in space, the fluctuating permittivity is a Gaussian random variable with zero mean and probability density function given by

$$P_{\varepsilon f}(\zeta) = \frac{1}{\sqrt{2\pi\delta}} \exp\left(\frac{-\zeta^2}{2\delta}\right). \tag{30}$$

The correlation function between the permittivities at two points is also given by a Gaussian function as follows:

$$C(\bar{r}_1 - \bar{r}_2) = \left\langle \varepsilon_f(\bar{r}_1)\varepsilon_f^*(\bar{r}_2) \right\rangle = \delta \exp\left(-\frac{|\bar{r}_1 - \bar{r}_2|^2}{l_s^2}\right). \tag{31}$$

The simulation is carried out using a two-dimensional FDTD with a uniform space discretization size of $\Delta_s = \lambda_s/10$. As antenna array 40 transceivers are used, spanning with inner spacing $d = \lambda_s/2$ and parallel to the x-axis. The UWB time domain excitation is the first derivative of Blackmann-Harris pulse [34] at $f = 1\,\text{GHz}$. The current source is located at the center of the domain setup and moves with constant velocity $v = c/10$ in $-y$ direction. The average relative dielectric permittivity is 5.5.

4.1. First-order Medium-statistics Effects

The effect of the variance of the random medium on the focusing properties of the time-reversed signals in the TM_z case is taken into consideration. The variance is changed from $\delta = 0.01\varepsilon_m$ to $\delta = 0.08\varepsilon_m$ while the correlation length is fixed at $l_s = 5\Delta_s$. The results of four different simulations are shown in Fig. 3, where the z-component of the electric field distribution (snapshot) is plotted at the time of refocusing. Fig. 4 shows the directivity pattern of the refocused field for different variances. It can be observed from the plot that as the variance increases, the spot size of the focused field is reduced, characterizing super resolution.

4.2. Second-order Medium-statistics Effects

Similar simulations are performed to assess the effect of different correlation lengths on the resolution for the case. The correlation
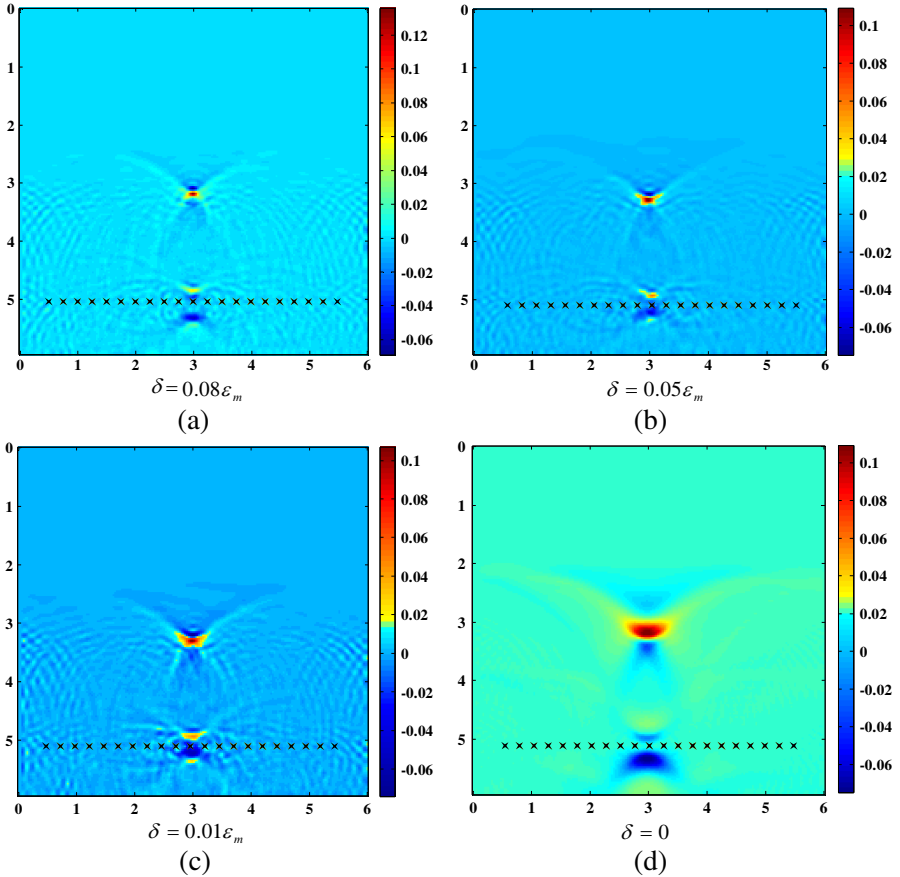
Figure 3. Spatial distribution of the time-reversed z-component of the electric field (E_z) at the time of refocusing when the variance (δ) of the random media is changed for fixed correlation length of $l_s = 5\Delta_s$.

length is changed from $l_s = 4\Delta_s$ to $l_s = 15\Delta_s$ for fixed variance of $\delta = 0.08\varepsilon_m$. Results are shown in Fig. 5, where it is seen that increasing the correlation length degrades the focusing properties.

5. DISCUSSION

Prior works on imaging non stationary objects using time reversal method are based on assumption of slowly varying targets in a sense that frequency distortion of transmitting signal could be neglected [25]. Therefore the time reversal operator decomposition (DORT) [8, 16],
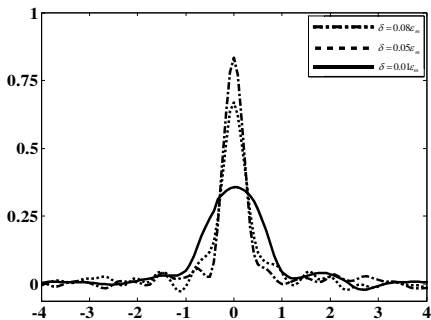
Figure 4. The directivity pattern of the refocused E_z components for the simulations in Fig. 3 where the field intensity is plotted at $x = x_s$ (range) with respect to the transverse y-coordinate (cross-range).
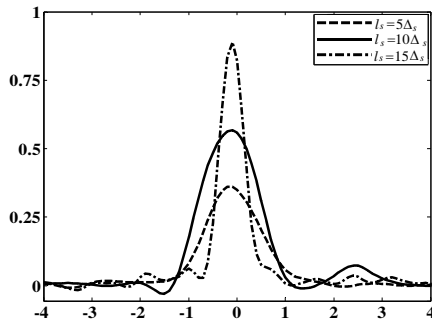
Figure 5. The directivity pattern of the refocused E_z components for the when the correlation length of the random medium is changed for fixed of $\delta = 0.08\varepsilon_m$.

and the time reversal multiple signal classification (TR-MUSIC) [15], which are frequency based methods, can be implemented. Although this is not the case in general and methods based on frequency domain processing fail due to Doppler frequency shift. Thus, in this paper time reversal focusing of uniformly moving target is investigated via time domain analysis. Equation (29) shows that focusing of time reversed fields is achievable in non stationary targets and time reversal imaging can detect moving target location. This method is not limited to homogeneous media and its performance in continues random media is investigated in this paper.

6. CONCLUSION

Time reversal focusing of electromagnetic waves is investigated in case of source motion. Analytical formulation of time reversed electric field due to uniformly moving source is extracted. Numerical simulation is performed via FDTD to support analytical results which shows that in case of moving point source spatial focusing is still achievable. Furthermore, Effects of background clutter from continuous random media on focusing properties of non stationary source is investigated. Similar to the standard case, it has been observed that an increase in multiple scattering effects leads to better focusing resolution of the time-reversed signals.

REFERENCES

1. Fink, M., "Time reversed acoustics," *Physics Today*, Vol. 50, No. 3, 34–40, 1997.

2. Lerosey, G., J. de Rosny, A. Tourin, A. Derode, G. Montaldo, and M. Fink, "Time reversal of electromagnetic waves," *Physical Review Letters*, Vol. 92, No. 19, 193904-1, 2004.

3. Ge, G.-D., D. Wang, and B.-Z. Wang, "Subwavelength array of planar triangle monopoles with cross slots based on far-field time reversal," *Progress In Electromagnetics Research*, Vol. 114, 429–441, 2011.

4. Liu, X.-F., B.-Z. Wang, and S.-Q. Xiao, "Electromagnetic subsurface detection using subspace signal processing and half-space dyadic Green's function," *Progress In Electromagnetics Research*, Vol. 98, 315–331, 2009.

5. Davy, M., J.-G. Minonzio, J. de Rosny, C. Prada, and M. Fink, "Influence of noise on subwavelength imaging of two close scatterers using time reversal method: Theory and experiments," *Progress In Electromagnetics Research*, Vol. 98, 333–358, 2009.

6. Chen, X., "Time-reversal operator for a small sphere in electromagnetic fields," *Journal of Electromagnetic Waves and Applications*, Vol. 21, No. 9, 1219–1230, 2007.

7. Liu, X.-F., B.-Z. Wang, S.-Q. Xiao, and J. H. Deng, "Performance of impulse radio UWB communications based on time reversal technique," *Progress In Electromagnetics Research*, Vol. 79, 401–413, 2008.

8. Tortel, H., G. Micolau, and M. Saillard, "Decomposition of the time reversal operator for electromagnetic scattering," *Journal of Electromagnetic Waves and Applications*, Vol. 13, No. 5, 687–719, 1999.

9. Xiao, S.-Q., J. Chen, B.-Z. Wang, and X.-F. Liu, "A numerical study on time-reversal electromagnetic wave for indoor ultra-wideband signal transmission," *Progress In Electromagnetics Research*, Vol. 77, 329–342, 2007.

10. Zhai, H., S. Jung, and M. Lu, "Wireless communication in boxes with metallic enclosure based on time-reversal ultra-wideband technique: A full-wave numerical study," *Progress In Electromagnetics Research*, Vol. 101, 63–74, 2010.

11. Xiao, S.-Q., J. Chen, X.-F. Liu, and B.-Z. Wang, "Spatial focusing characteristics of time reversal UWB pulse transmission with different antenna arrays," *Progress In Electromagnetics Research B*, Vol. 2, 223–232, 2008.

12. Mao, X., D.-Y. Zhu, and Z.-D. Zhu, "Signatures of moving target in polar format spotlight SAR image," *Progress In Electromagnetics Research*, Vol. 92, 47–64, 2009.

13. Tian, B., D.-Y. Zhu, and Z.-D. Zhu, "A novel moving target detection approach for dual-channel SAR system," *Progress In Electromagnetics Research*, Vol. 115, 191–206, 2011.

14. Mao, X., D.-Y. Zhu, L. Ding, and Z.-D. Zhu, "Comparative study of rma and pfa on their responses to moving target," *Progress In Electromagnetics Research*, Vol. 110, 103–124, 2010.

15. Bellomo, L., S. Pioch, M. Saillard, and E. Spano, "Time reversal experiments in the microwave range: Description of the radar and results," *Progress In Electromagnetics Research*, Vol. 104, 427–448, 2010.

16. Zheng, W., Z. Zhao, and Z.-P. Nie, "Application of TRM in the UWB through wall radar," *Progress In Electromagnetics Research*, Vol. 87, 279–296, 2008.

17. Zheng, W., Z. Zhao, Z.-P. Nie, and Q. H. Liu, "Evaluation of TRM in the complex through wall environment," *Progress In Electromagnetics Research*, Vol. 90, 235–254, 2009.

18. Zhang, W., A. Hoorfar, and L. Li, "Through-the-wall target localization with time reversal music method," *Progress In Electromagnetics Research*, Vol. 106, 75–89, 2010.

19. Davy, M., T. Lepetit, J. de Rosny, C. Prada, and M. Fink, "Detection and imaging of human beings behind a wall using the DORT method," *Progress In Electromagnetics Research*, Vol. 110, 353–369, 2010.

20. Zhu, X., Z. Zhao, W. Yang, Y. Zhang, Z.-P. Nie, and Q. H. Liu, "Iterative time-reversal mirror method for imaging the buried object beneath rough ground surface," *Progress In Electromagnetics Research*, Vol. 117, 19–33, 2011.

21. Higley, W. J., P. Roux, W. A. Kuperman, W. S. Hodgkiss, H. C. Song, T. Akal, and M. Stevenson, "Synthetic aperture time-reversal communications in shallow water: Experimental demonstration at sea," *Journal of Acoustical Society of America*, Vol. 118, No. 4, 2365–2372, 2005.

22. Gomes, J. and V. Barroso, "Doppler compensation in underwater channels using time-reversal arrays," *IEEE International Conference on Acoustics Speech and Signal Processing*, 81–84, Hong Kong, China, 2003.

23. Jackson, D. R. and D. R. Dowling, "Phase conjugation in underwater acoustics," *Journal of Acoustical Society of America*,

Vol. 89, No. 1, 171–181, 1990.

24. Yuanwei, J., J. M. F. Moura, N. O'Donoughue, and J. Harley, "Single antenna time reversal detection of moving target," *IEEE International Conference on Acoustics Speech and Signal Processing*, 558–3561, 2010.

25. Fouda, A. E. and F. L. Teixeira, "Imaging and tracking of targets in clutter using differential time-reversal techniques," *Waves in Complex and Random Media*, Vol. 22, No. 1, 1–43, 2012.

26. De Rosny, J., G. Lerosey, and M. Fink, "Theory of electromagnetic time-reversal mirrors," *IEEE Transactions on Antennas and Propagation*, Vol. 58, No. 10, 3139–3149, 2010.

27. Yavuz, M. E. and F. L. Teixeira, "A numerical study of time-reversed UWB electromagnetic waves in continuous random media," *IEEE Antennas and Wireless Propagation Letters*, Vol. 4, 43–46, 2005.

28. Yavuz, M. E. and F. L. Teixeira, "Full time-domain DORT for ultra wideband electromagnetic fields in dispersive, random inhomogeneous media," *IEEE Transactions on Antennas and Propagation*, Vol. 54, No. 8, 2305–2315, 2006.

29. Cassereau, D. and M. Fink, "Time-reversal of ultrasonic fields. III. Theory of the closed time-reversal cavity," *IEEE Transactions on Ultrasonics, Ferroelectrics and Frequency Control*, Vol. 39, No. 5, 579–592, 1992.

30. Carminati, R., R. Pierrat, J. de Rosny, and M. Fink, "Theory of the time reversal cavity for electromagnetic fields," *Opt. Lett.*, Vol. 32, No. 21, 3107–3109, 2007.

31. Felsen, L. B. and N. Marcuvitz, *Radiation and Scattering of Waves*, Prentice-Hall, New Jersey, 1973.

32. De Rosny, J. and M. Fink, "Focusing properties of near-field time reversal," *Physical Review A*, Vol. 76, No. 6, 2007.

33. Moss, C. D., F. L. Teixeira, Y. E. Yang, and J. A. Kong, "Finite-difference time-domain simulation of scattering from objects in continuous random media," *IEEE Transactions on Geoscience and Remote Sensing*, Vol. 40, No. 1, 178–186, 2002.

34. Harris, F. J., "On the use of windows for harmonic analysis with the discrete fourier transform," *Proceedings of the IEEE*, Vol. 66, No. 1, 51–83, 1978.